Measurement Principle for Measuring High Frequency Bearing Currents in Electric Machines and Drive Systems

Benjamin Knebusch, Lennart Jünemann, Pauline Höltje, Axel Mertens and Bernd Ponick
Leibniz University Hannover
Institute of Drive Systems and Power Electronics
Welfengarten 1
30167 Hannover, Germany
Phone: +49 511-762 2408
Fax: +49 511 762 3040
Email: benjamin.knebusch@ial.uni-hannover.de
URL: https://www.ial.uni-hannover.de

Keywords

≪Bearing currents≫, ≪Component for measurements≫, ≪Impedance measurement≫

Abstract

In this paper, a new principle for measuring bearing currents will be presented and validated using a replica of a drive system. The idea is to insulate the bearing and create a new current path on a PCB for the bearing current, together with a defined impedance in that path.

Introduction

Electric motors powered through frequency converters are increasingly being used in modern drive systems. Modern frequency inverters - especially with wide-bandgap (WBG) power semiconductors - use high voltage gradients, which enable dynamic operation with both low switching losses and smaller passive components. This leads to electrical voltages across bearings and other machine elements, which can result in bearing currents. Machine elements that are subjected to critical electrical stress can be massively damaged. This can lead to the failure of the affected component, the subcomponent or the entire system.

Various studies exist regarding the analytical prediction of the electrical stress on bearings and other machine elements [1, 2, 3, 4, 5, 6]. However, for the validation of these approaches, it is necessary to compare the calculations to measurements. The challenge with this measurement is that the electrical structure of the overall system should not be changed significantly by the insertion of the measuring tools.

In this paper, a methodology for measuring the electrical current through bearings is presented and validated. After a brief introduction to the origin of bearing currents in section *High Frequency bearing currents*, the general measuring principle for bearing currents is presented in section *Explanation of the measuring principle*. The rest of this section provides a description of the structure of a measurement board. For the validation of this measurement methodology, the construction of the circuit board developed and its installation in a bearing replica are explained in section *Design of the test bench*. The results of the measurement are given in section *Results* and are compared with two other measurements.

High frequency bearing currents

WBG power semiconductors offer a number of advantages in comparison to conventional silicon power semiconductors. The use of silicon carbide (SiC) semiconductors increases the possible voltage gradient $\mathrm{d}u/\mathrm{d}t$ by about one order of magnitude. This reduces losses, but causes critical high frequency excitations and increases the common mode currents through parasitic capacitances.

A distinction is made between circular and electric discharge machining (EDM) bearing currents. Circular bearing currents are due to capacity current flow across the parasitic capacitance between the stator lamination and the winding. This creates a circular magnetic field in the stator yoke, which induces a voltage in the conductor loop of the rotor shaft, bearing, end shields and housing, causing a current to flow.

EDM bearing currents are the result of the galvanic separation of winding, stator and rotor. The common mode voltage U_{CM} ingressed to the stator winding excites a capacitive voltage divider across the entire drive, as shown in Figure 1. The resulting electric voltage across the bearings is calculated using the bearing voltage ratio

$$f_{\mathrm{BVR}} = \frac{C_{\mathrm{WR}}}{C_{\mathrm{WR}} + C_{\mathrm{DE}} + C_{\mathrm{NDE}} + C_{\mathrm{RS}}} \tag{1}$$

which results in a bearing voltage of

$$U_{\mathrm{B}} = U_{\mathrm{CM}} \cdot f_{\mathrm{BVR}}. \tag{2}$$

A third high frequency bearing current phenomenon is called rotor-ground currents. On systems where the ground impedance between motor and inverter has its lowest path through the system attached to the shaft, the common-mode (CM) current will most likely take its path through the shaft and therefore directly through one or more bearings.

In order to measure the bearing current, a defined path for the bearing current is necessary to apply a valid measurement probe. Common practice, the bearings stationary part is insulated from the bearing shield and a wire or litz-wire is used to close the loop and attach a current sensor [7]. This type of application will force the current to take a completely different current path and will have an unknown impact on the overall current path impedance. Another method is the application of one or several rogowski coils around the shaft as shown in [8], the downside of this being the limited bandwith of the rogowski coils.

The presented system will overcome both downsides: On the one hand, the current path will stay symmetrical, and the known input impedance will help to validate simulations with measurements, and, on the other hand, the target bandwidth will be higher than 40 MHz.

Explanation of the measuring principle

This section deals with the general procedure for measuring bearing currents and with the implementation of the new concept using an integrated measuring PCB.

General Measurement of Bearing Currents

To measure a bearing current, it must flow along a defined path through a probe. To do this, all potential paths for the bearing current must be identified and then prevented by insulation. Figure 1 shows a motor with a housing, two bearings and the rotor shaft. The bearings need to be insulated by a nonconducting sleeve as the first step. It must be ensured that the additional capacitance does not - relatively to the other capacitances in the machine - become significantly large, in order to prevent an influence on f_{BVR}. However, a sufficiently thick insulation layer must be employed to prevent an insulation breakdown. With these modifications, the circuit is interrupted. The current is now conducted over a defined measuring path from the bearing outer ring to the housing. In order to be able to investigate the electrical stress of each bearing individually, it must be possible to detach or switch off the measuring path. The EDM bearing stress is determined by measuring the bearing current via the measuring path. This is performed individually for each bearing. To clearly identify the circular current in the system, the insulation of all bearings or at least two which encircle the circular flux have to be bridged. This also includes EDM bearing currents if they occur. Depending on the condition of each bearing, one or the other type of bearing current will dominate.

Design of the measuring PCB

In this section, the measuring board, which functions as a measuring path, is presented. The measuring principle is based on acquiring the voltage over a shunt resistor [9]. Using the measured voltage and a

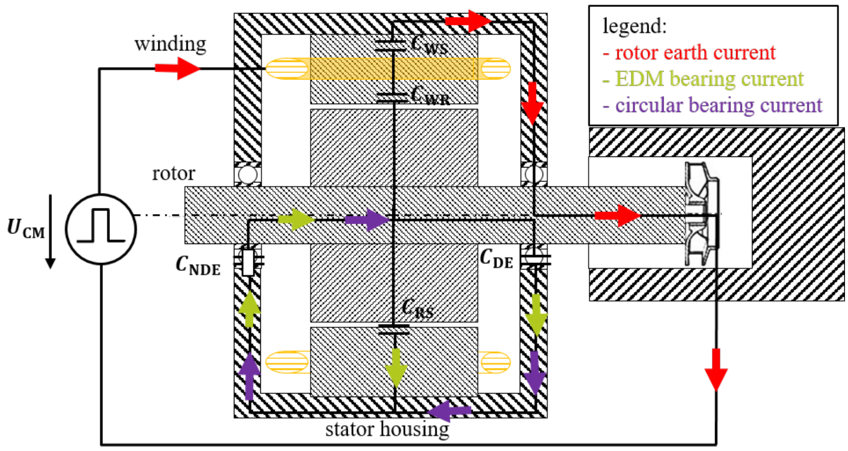

Fig. 1: Distinction of Different Kinds of Bearing Current

known impedance value, the current can be calculated. The current is picked up on the bearing outer race via contact pins. Contact probe tips from the manufacturer Ingun (GKS-913305230A2502Z) are used. The shunt is placed on the measuring board, with the electric voltage being measured at both sides of the shunt. The current is then conducted back to the housing through relays [10]. The relays are responsible for manually switching off each circuit board in order to measure the bearings in the drive individually.

Care must be taken to ensure that all components are distributed as evenly as possible radially around the circumference to ensure an equipotential surface and thus reduce measurement inaccuracies. This direct measurement concept at the bearing offers the advantage that the current does not have to be conducted to the outside via a high impedance path, which often leads to severely compromised results. Furthermore, the effort of rebuilding the machine is also much lower. In [11], a large part of the machine is milled off to get to the bearing, which also leads to a modification in the system. The novel measuring board is barely larger than the bearing itself and takes up only a few millimeters of axial length in the machine. With this concept, even in machines close to series production, only minor changes are necessary for the implementation of the measuring PCB. Even if it is possible to use this methode in close to series production drives, a measurement of bearing currents in a series drive is not meaningful. In addition, the measurement methodology is much less expensive than measuring with high-precision probes. It can also be used without the probe tips directly mounted between two isolated surfaces in a machine.

Selection of components

Due to the high frequencies of the bearing currents, it is indispensable to produce a structure that is as clean as possible. Therefore it is important to select the components accordingly. However, there must be a trade-off between high frequency capability and component size, since there is not much installation space for additional components in most e-machines. The shunt also needs to be able to withstand a certain load, since the bearing current can reach several amperes.

The shunt selected here is a 40.2 Ω high frequency thin film chip resistor in a 0402 package from Vishay [9]. This exhibits purely resistive behavior into the gigahertz range. There are 60 resistors evenly connected in parallel around the circumference. Thus, the effective resistance is 670 mΩ. It is necessary to achieve a low resistance value, so that there is no significant impact on the value of the bearing current.

To pick up the bearing current from the bearing outer race, pins contact the outer race as evenly as possible. The contact pins are made of beryllium copper with a gold coating. Again, the focus here is on the current carrying capability and a low impedance that is as independent of frequency as possible. Depending on the length, the contact pins have an internal resistance of 100 mΩ. The relays are Panasonic AQV255GS [10]. These relays, switching via optocouplers, have a small size and a low parasitic capacitance. A parallel connection ensures an even current distribution. U.FL connectors are used to control the relays and to measure the voltage across the shunt. These also have a low physical volume.

Measurement Methodology

The voltage right before and after the shunt is tapped relative to a separate measuring ground. This offers the advantage that the measurement is independent of the housing's local potential, which normally acts as the measuring ground. However, due to currents in the housing, a potential shift can occur, which compromises the measurement results.

The control for the relays is also located on a separate PCB layer to keep the control as decoupled as possible from the measurement to avoid electromagnetic interference. Figure 2 shows the top layer of the PCB. On this layer, the contact pins pick up the current from the bearing. These are mounted in retaining bushes. Furthermore, the relays are visible on this side. The shunts and U.FL connections are located on the bottom layer.

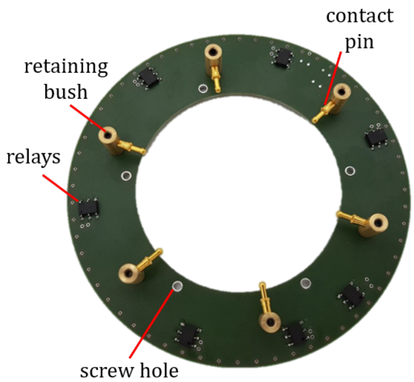

Fig. 2: Measuring circuit board

Design of the test bench

This section deals with the design of the test bench. First, the replica of the e-machine is explained. Subsequently, further components for carrying out the test are presented.

Replica of the e-machine

In order to validate the measurement concept, the most important components of the an e-machine are reproduced to simulate the assembly and installation work. The system setup for this purpose is shown in Figure 3. The replica consists of a shaft onto which a 6008 ball bearing is pressed. As described above, this must be isolated from the rest of the machine, so that an insulating sleeve is fitted over the bearing outer race. This is followed by the housing, which has recesses in which the contact pins of the axially mounted PCB are located.

To validate the measurements, a passive current sensor is integrated around the shaft to determine the current flowing in various subsequent measurements. This is completed by the end shield and a BNC connector through which the current is supplied to the e-machine replica.

The shaft is also isolated from the housing. So the resulting current path begins on the signal line of the BNC connector, flows through the shaft, through the bearing to the PCB and through the screw back to the ground line of the BNC connector on the housing. This path is now very simular to the path of the real bearing current in an e-machine.

Experimental procedure

The test bench is shown in Figure 4. The test bench consists of the bearing replica, the control system belonging to the measuring board - consisting of microcontroller and control board - a power supply, a signal generator, three different measuring sensors and two oscilloscopes. The second oscilloscope, a Keysight Technologies InfiniiVision MSO7104A [12], is used to display the signal from the high frequency sensor. The voltage source is used to switch on the relays by supplying a voltage to the optocoupler. The circuit is then enabled by the microcontroller which connects the power circuit through

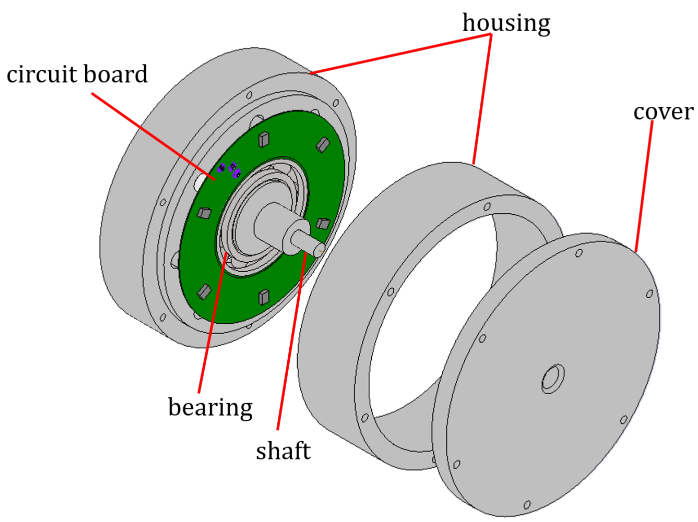

Fig. 3: Assembly of the e-machine replica

the MOSFET. The signal generator - AimTTi TGA12100 - is directly connected to the BNC terminal of the replica. A sinusoidal voltage with an amplitude of 10 V at various frequencies up to a maximum of 40 MHz is applied.

The first current measurement is performed on the shaft of the replica with a high precision HF Current Transformer CT-D1.0-B from AMS technologies (passive sensor). There is a small axial preload on the bearing to ensure that the bearing is electrically conductive at standstill, the voltage drops across shaft, bearing, contact pins, PCB and finally the screw connection back to the housing.

The high frequency differential voltage probe 1134A 7 GHz InfiniiMax from Keysight Technologies measures the voltage difference across the shunts on the PCB. In addition, two U.FL connectors measure the electrical potential before and behind the shunts relative to a defined measurement ground on the other side of the board. The cables of the three sensors are fed through a hole in the housing to the oscilloscope, which is a Teledyne LeCroy HDO8108A. This determines the voltage difference between the two U.FL connectors. The second oscilloscope - which is pictured in the figure - serves to display the HF sensor.

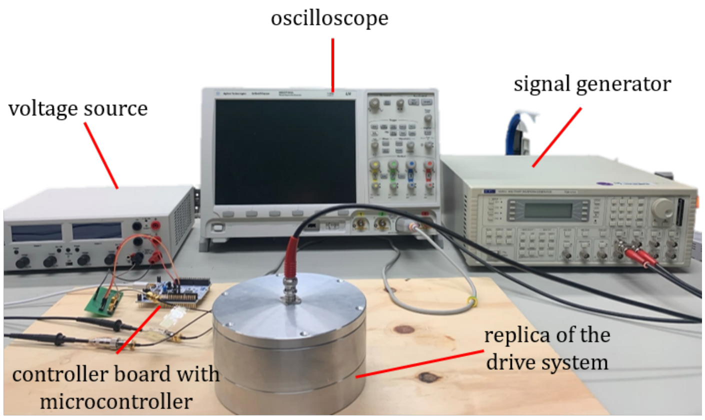

Fig. 4: Test bench

Results

In this section, the results of the impedance measurement are presented first, and these can be used to determine the currents corresponding to the measured voltages. Then, the results of the current measurements at different frequencies are shown.

Measurement of the impedance

The impedance of the measurement board was recorded with a Wayne Kerr 65120B. Since only U.FL connections are integrated onto the board, an adapter cable from U.FL to BNC connection was also used; therefore, the impedance of the cable was determined in a second measurement. Thus, the results of the board measurement including the adapter cable could be corrected for the influences of the cable. In Figure 5, the measured resistance of the board is shown against the frequency. Up to a frequency of 20 MHz, the resistance of the board is constant at 690 mΩ. Beyond this point, the resistance increases with increasing frequency. At a frequency of 96 MHz, the resistance is 2.6 Ω. Above this frequency, the resistance decreases with increasing frequency due to parasitic capacitive couplings. This drop is most probably to be due to resonance in the cable.

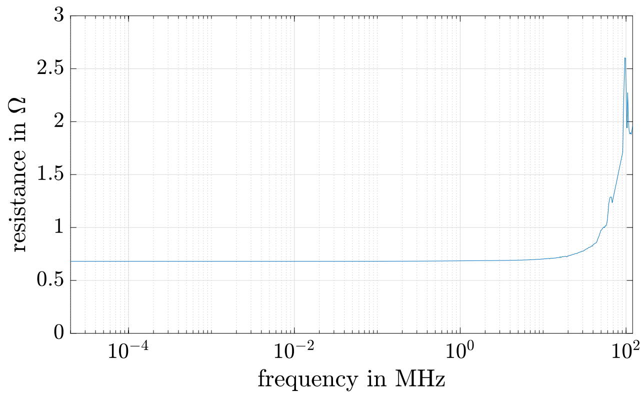

Fig. 5: Frequency-dependent shunt resistance

For the validation of the system and measuring at constant frequency, the impedance curve can be interpolated and the corresponding impedance can be used to calculate the bearing current from the measured voltages using

$$i_{\text{bearing}} = \frac{u_{\text{shunt}}}{|\underline{Z}_{\text{shunt}}(f)|}. \tag{3}$$

When measuring transient currents in real drive systems a post processing is necessary. Therefore the measured shunt voltage is transformed in the frequency domain

$$u(t) \xleftrightarrow{\mathcal{F}} \underline{U}(f). \tag{4}$$

The impedance curve is also interpolated to the sampling points of the FFT in magnitude and phase, and the corresponding current components for each frequency are calculated using

$$\underline{I}_{\text{bearing}}(f) = \frac{\underline{U}_{\text{shunt}}(f)}{\underline{Z}_{\text{shunt}}(f)}. \tag{5}$$

The result is then back-transformed into time domain

$$\underline{I}_{\text{bearing}}(f) \xleftrightarrow{\mathcal{F}^{-1}} i_{\text{bearing}}(t) \tag{6}$$

to get the corresponding transient signal.

Current measurement

The results of the three different measurement methods with the passive current sensor (current sensor), the HF voltage differential probe (HF sensor) and the differential measurement using the U.FL connectors at shunts (shunt) will now be compared to each other. To determine the currents, the measured voltage differences from the HF sensor and the U.FL connectors are divided by the frequency-dependent board resistance. Figure 6 shows the measured currents as a function of time for a sinusoidal voltage with a frequency of 1 MHz, provided by the signal generator. All three measurement methods identify the

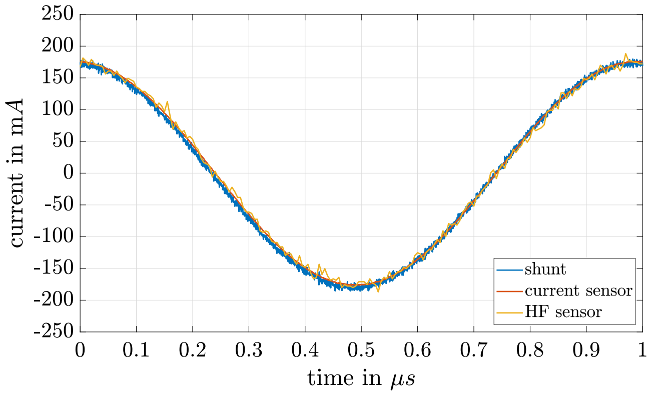

Fig. 6: Measured currents at a frequency of 1 MHz

same current with an amplitude of approximately 170 mA. Even at a frequency of 10 MHz, as shown in Figure 7, the currents measured with the three methodologies correspond well to each other. Some deviations exist between the three curves, which can be traced back to parasitic effects. The amplitudes are slightly different, because of different voltage supplies.

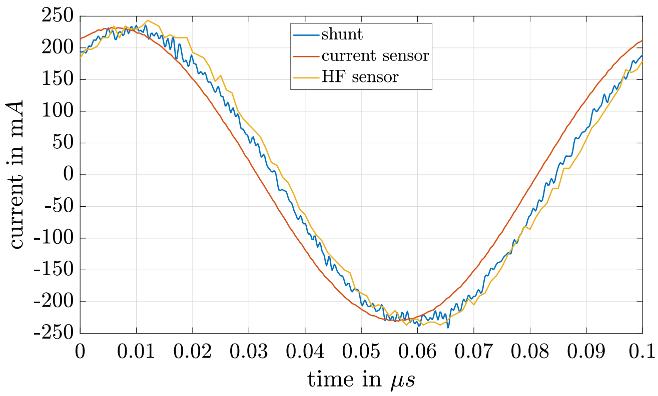

Fig. 7: Measured currents at a frequency of 10 MHz

Figure 8 compares the results for a supply with a frequency of 40 MHz. The current sensor on the shaft measures the highest current with an amplitude of almost 197 mA. In comparison, the shunt measurement records an amplitude of 186 mA and the HF sensor only 151 mA. The current sensor measures the total current flowing through the shaft, but the shunts and the HF sensor only capture the current on the measuring PCB.

Due to parasitic capacitances within the experimental setup, it can be assumed that not the total current flows across the PCB, as some of the current is diverted towards the housing. The differences between the shunt and the HF sensor measurements are due to the different connecting leads. In order to connect the HF sensor to the PCB, short pieces of wire were soldered on which the sensor sticks to. Even if these connecting wires are kept as short as possible, they create a conductor loop which slightly distorts the measurement.

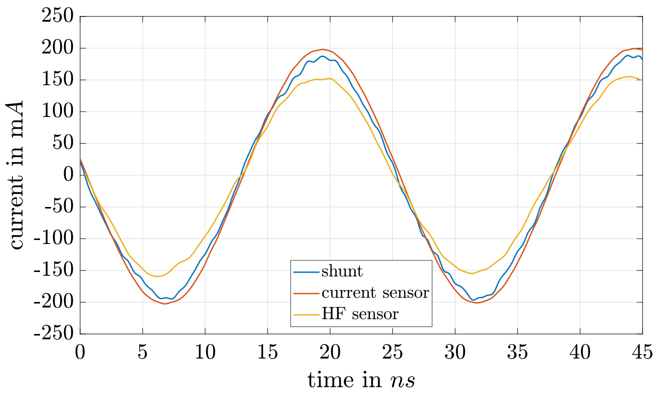

Fig. 8: Measured currents at a frequency of 40 MHz

Conclusion

In this paper, a novel PCB for measuring bearing currents, intended to allow measuring bearing currents in real drive systems with much lower modification effort compared to the state of art, is presented and validated with the help of a simplified example measurement. For the measurement, it is necessary to electrically isolate the bearing from the housing and only allow a current flow along a defined path via a measuring PCB. On the measuring PCB, the current is determined from the voltage drop across shunts. The measuring PCB can be switched on and off using relays. The measurement principle designed here was tested on a simplified e-machine replica and validated against two other measurement methods for frequencies up to 40 MHz. In a future study, the principle will also be tested at higher frequencies. Furthermore, the PCB will be integrated and tested in a real e-machine.

Acknowledgement

The basic concept for measuring high-frequency bearing currents with circumferentially arranged shunt resistors was proposed by Urs Obernolte of Lenze SE and is part of the project UmSiCht, funded by the Federal Ministry for Education and Research on the basis of a decision by the German Bundestag. Funding number: 16EMO0252.

References

[1] B. J. Hamrock, D. Dowson, and T. Tallian, *Ball bearing lubrication: The elastohydrodynamics of elliptical contacts*. NASA National Aeronautics and Space Administration, 1982.

[2] A. Furtmann, H. Tischmacher, and G. Poll, "Extended hf equivalent model of a drive train," in *2016 XXII International Conference on Electrical Machines (ICEM)*. IEEE, 2016, pp. 2244–2250.

[3] E. Wittek, M. Kriese, H. Tischmacher, S. Gattermann, B. Ponick, and G. Poll, "Capacitances and lubricant film thicknesses of motor bearings under different operating conditions," in *The XIX International Conference on Electrical Machines-ICEM 2010*. IEEE, 2010, pp. 1–6.

[4] Y. Gemeinder, M. Schuster, B. Radnai, B. Sauer, and A. Binder, "Calculation and validation of a bearing impedance model for ball bearings and the influence on edm-currents," in *2014 International Conference on Electrical Machines (ICEM)*. IEEE, 2014, pp. 1804–1810.

[5] M. Schuster and A. Binder, "Comparison of different inverter-fed ac motor types regarding common-mode bearing currents," in *2015 IEEE Energy Conversion Congress and Exposition (ECCE)*. IEEE, 2015, pp. 2762–2768.

[6] H. Tischmacher, *Systemanalysen zur elektrischen Belastung von Wälzlagern bei umrichtergespeisten Elektromotoren*. Hannover: Gottfried Wilhelm Leibniz Universität Hannover, 2017.

[7] A. Muetze and A. Binder, "Techniques for measurement of parameters related to inverter-induced bearing currents," *IEEE transactions on industry applications*, vol. 43, no. 5, pp. 1274–1283, 2007.

[8] A. E. B. P. D. Heide, B. Knebusch, , *"Measurement of Parasitic High-Frequency Currents in Inverter-Fed Low-Speed Electrical Machines Using Rogowski Current Sensors*. 23rd European Conference on Power Electronics and Applications (EPE'21 ECCE Europe), 2021.

[9] *High Frequency 50 GHz Thin Film Chip Resistor*, Vishay, 2020, revised 10.2021.

[10] *PhotoMOS - Miniature SOP6-pin type with high capacity of 3A load current*, Panasonic Industry, 2020, revised 10.2021.

[11] A. M. Bubert, *Optimierung des elektrischen Antriebsstrangs von Elektrofahrzeugen mit Betrachtung parasitärer Ströme innerhalb der elektrischen Maschine*. Aachen: RWTH Aachen Universität, Aachener Beiträge der ISEA, Band 141, 2020.

[12] *Infiniium Oscilloscope Probes and Accessories*, Keysight Technlogies, 2021, revised 10.2021.